

# Resonance states of ${}^5\text{H}$ and ${}^5\text{Be}$ in a microscopic three-cluster model

Koji Arai\*

*Department of Physics, University of Surrey, Guildford GU2 7XH, United Kingdom*

(Received 19 May 2003; published 5 September 2003)

Resonance states of  ${}^5\text{H}$  and  ${}^5\text{Be}$  have been studied using microscopic  $t+n+n$  and  $h+p+p$  three-cluster models, respectively. The resonance positions are localized by the three-body complex scaling method. An effective nucleon-nucleon interaction, which reproduces the  $\alpha+N$  low energy phase shifts and the energies of the  $0^+$  ground and  $2^+$  first excited states of  ${}^6\text{He}$  with the three-cluster model, is used to calculate resonance states of  ${}^5\text{H}$  and  ${}^5\text{Be}$ . This model can reasonably reproduce the experimental  $t+n$  and  $h+p$  phase shifts at low energies. It gives a  $1/2^+$  broad resonance as the ground state in  ${}^5\text{H}$  and  ${}^5\text{Be}$  and in addition it gives two excited resonance states of  $3/2^+$  and  $5/2^+$ . The resonance parameters of the  $1/2^+$  state of  ${}^5\text{H}$  in the present model are close to those deduced from their recent experimental data by Korshennikov *et al.* The same effective nucleon-nucleon interaction is used for a tentative investigation in order to explore the possibility of a tetra-neutron ( ${}^4n$ ) resonance by means of the  $n+n+n+n$  four-body complex scaling method on a restricted set of model configurations. Our model does not give any evidence for a tetra-neutron resonance.

DOI: 10.1103/PhysRevC.68.034303

PACS number(s): 27.10.+h, 21.10.Dr, 21.60.Gx

## I. INTRODUCTION

Recent developments in the experimental techniques of nuclear radioactive beams have highlighted exotic structures in certain light unstable nuclei [1]. One example is the neutron halo structure which is found in some light neutron-rich nuclei. The  ${}^6\text{He}$  system is one of the neutron halo nuclei and has a good  $\alpha+n+n$  three-body structure (i.e., a borromean system) with a small binding energy of  $E = -0.973$  MeV for the ground state with respect to the three-body threshold [2]. Since protons are distributed only inside the core in the neutron halo nucleus, it is very intriguing to ask the question: “How does this structure change if the proton number inside the core is changed?” In the case of  ${}^6\text{He}$ , two protons occupy states inside the  $\alpha$  particle, and if one proton is removed then this system turns to  ${}^5\text{H}$  with the  $t+n+n$  three-cluster system. This  ${}^5\text{H}$  nucleus is studied in this paper. Here the core nucleus, the triton (with a binding energy  $E = -8.48$  MeV [3]), is a well bound nucleus but is not strongly rigid like the  $\alpha$  particle ( $E = -28.30$  MeV [3]). The binding is sufficient so that it seems to be valid to employ the  $t+n+n$  three-cluster model for  ${}^5\text{H}$  and this can afford a discussion of this nucleus via a consistent model with  ${}^6\text{He}$ . According to this motivation, we adopt the same effective nucleon-nucleon interaction and a consistent model space compared to those that reproduce satisfactorily the structure of  ${}^6\text{He}$  by the three-cluster model.

The ground state of  ${}^6\text{He}$  has a well-known underbinding problem in a three-body model, as does  ${}^{11}\text{Li}$ . In order to overcome this problem the model space should be extended by including an additional  $t+t$  channel to the  $\alpha+n+n$  model [4]. However  ${}^5\text{H}$  cannot have such a two-body channel because two neutrons do not form a bound state. Further, since the triton has a much smaller binding energy than the  $\alpha$  particle, the core distortion effect in the three-cluster system

of  ${}^5\text{H}$  is expected to be more important than that in  ${}^6\text{He}$ , but the effect in  ${}^6\text{He}$  is important to reproduce the binding energy [5]. Therefore a detailed comparison of the three-cluster structure between  ${}^6\text{He}$  and  ${}^5\text{H}$  is likely to be very helpful in elucidating the binding mechanism in the neutron halo nucleus. However the ground state of  ${}^5\text{H}$  is not a particle-stable state and none of the binary subsystems form bound states. Therefore we need a three-body resonance treatment in order to study the  ${}^5\text{H}$  nucleus and also the excited states of  ${}^6\text{He}$ . This fact immediately makes the studies of  ${}^5\text{H}$  and  ${}^6\text{He}^*$  much more complicated. There have been a few theoretical studies in the framework of the three-body model to investigate these resonance states by means of the hyper-spherical harmonics method [6] and the analytical continuation in the coupling constant [7]. In this paper we employ the three-body complex scaling method (CSM) [8,9] in order to calculate the resonance states of  ${}^5\text{H}$  and  ${}^5\text{Be}$ , since this method has previously been applied successfully to calculate the three-body resonances in other light nuclei [10–13].

The ground state of  ${}^6\text{He}$  is the  $0^+$  state and there is a well-known  $2^+$  excited state at excitation energy  $E_x = 1.80$  MeV with a small width  $\Gamma_r = 0.11$  MeV [2]. Therefore, because the total angular momentum of the triton is  $1/2^+$ , the ground state of  ${}^5\text{H}$  is presumably  $1/2^+$  state and possibly there are at least two resonance excited states of  $3/2^+$  and  $5/2^+$ . Accordingly our study in  ${}^5\text{H}$  is concentrated on the  $1/2^+$ ,  $3/2^+$ ,  $5/2^+$  states in the present paper. Recent experimental results on  ${}^1\text{H}({}^6\text{He}, {}^2\text{He}){}^5\text{H}$  by Korshennikov *et al.* give a resonance at  $E_r = 1.7 \pm 0.3$  MeV with respect to the  $t+n+n$  threshold, with a width  $\Gamma_r = 1.9 \pm 0.4$  MeV, which could possibly be the  $1/2^+$  ground state of  ${}^5\text{H}$  [14]. Additionally, we also perform similar calculations for the mirror nucleus  ${}^5\text{Be}$  with an  $h+p+p$  three-cluster model, where  $h$  stands for  ${}^3\text{He}$ .

If two protons are removed from  ${}^6\text{He}$ , this system does not possess any proton and it becomes a four-neutron system. Recently this four-neutron system has attracted much attention due to a recent experimental report [15] which discusses

\*Email address: k.arai@surrey.ac.uk

the possibility of a bound tetraneutron ( ${}^4n$ ). There are already several experimental and theoretical studies to discuss a three-neutron resonance [16]. Since theoretical calculations [17] do not show any evidence of the four-neutron bound state, it is an important question whether or not the four-neutron system has a four-body resonance state (the two- and three-neutron systems do not have bound states [3]). However it is not easy to calculate the four-body resonance accurately, and therefore we apply the complex scaling method to this four-neutron system but with the same effective nucleon-nucleon interaction used in  ${}^6\text{He}$  and with a restricted set of model configurations compared to  ${}^6\text{He}$ .

## II. MODEL

The microscopic multicluster model according to the resonating group method (RGM) [18,19] is used here. In this model the nucleus is assumed to consist of  $0s$  clusters. The total wave function satisfies the Pauli principle exactly for all nucleons, is free from the center-of-mass motion, and has good total angular momentum and parity. The intrinsic wave functions of the constituent clusters are taken to be simple shell model wave functions built up from  $0s$  harmonic-oscillator states. The wave function in the  $N$ -cluster system with total angular momentum  $J$  and parity  $\pi$  is given as

$$\Psi^{JM\pi} = \sum_{\lambda} C_{\lambda} \mathcal{A} \{ [\Phi_S^{\mu} [\Gamma_{\ell_1}(\nu_{k_1}, \mathbf{p}_1) \Gamma_{\ell_2}(\nu_{k_2}, \mathbf{p}_2) \cdots \Gamma_{\ell_{N-1}}(\nu_{k_{N-1}}, \mathbf{p}_{N-1})] ]_{JM} \}, \quad (1)$$

where the subscript  $\lambda$  stands for the set of labels  $\{\mu, S, (\ell_1, \ell_2, \dots, \ell_{N-1})L, K\}$ , and  $\mu$  specifies the different Jacobi arrangements. The parameter  $\nu_{k_i}$  determines the size of the tempered Gaussian function  $\Gamma_{\ell_i}(\nu_{k_i}, \mathbf{p}_i)$  [20] and  $K \equiv \{k_1, k_2, \dots, k_{N-1}\}$  labels the terms of the basis set. The symbol  $\mathcal{A}$  is the intercluster antisymmetrizer. The function  $\Phi_{SM_S}^{\mu}$  is the product of the cluster intrinsic wave functions where  $S$  is the total spin of the  $N$ -cluster system. The numbers  $\ell_1, \ell_2, \dots, \ell_{N-1}$  are the orbital angular momenta on the respective Jacobi coordinates  $\mathbf{p}_1, \mathbf{p}_2, \dots, \mathbf{p}_{N-1}$ . The coefficient  $C_{\lambda}$  is obtained by approximately solving the  $A$ -nucleon Schrödinger equation in which the Hamiltonian is given as

$$\hat{H} = \sum_{i=1}^A \hat{T}_i - \hat{T}_{\text{c.m.}} + \sum_{i < j} \hat{V}_{i,j}, \quad (2)$$

where  $\hat{T}_i$  is the kinetic energy of  $i$ th nucleon,  $\hat{T}_{\text{c.m.}}$  is the kinetic energy of the center-of-mass, and  $\hat{V}_{i,j}$  is the effective nucleon-nucleon interaction. The Minnesota force [21] with the Coulomb force is chosen as the central part of the effective nucleon-nucleon interaction and the Reichstein-Tang force (set number IV) [22] is added as the spin-orbit term. The tensor term, as usually with the Minnesota force, is not included in our Hamiltonian and the Minnesota force reproduces the deuteron binding energy without the  ${}^3D_1$  component. This potential has been employed to study the ground

and excited states of  ${}^6\text{He}$  with the microscopic cluster model [4,10] and reproduces fairly well the energies of the  $0^+$  and  $2^+$  states and the halo structure in the ground state. The core internal wave function should strictly be given as a superposition of several  $0s$  functions with different size parameters. However, owing to a limitation of the computer capacity we compromise and employ a single  $0s$  function in which the size parameter is chosen to minimize the energies of the  $\alpha$  particle and triton. The fitted values are  $\nu_{\alpha} = 0.303 \text{ fm}^{-2}$  for the  $\alpha$  particle and  $\nu_t = \nu_h = 0.2255 \text{ fm}^{-2}$  for the triton and  ${}^3\text{He}$ . These values give the binding energies  $-24.69$ ,  $-4.56$ , and  $-3.79 \text{ MeV}$  for the  $\alpha$  particle, triton, and  ${}^3\text{He}$ , respectively, while the corresponding experimental data are  $-28.30 \text{ MeV}$ ,  $-8.48 \text{ MeV}$ , and  $-7.72 \text{ MeV}$  [3]. The exchange mixture parameter  $u$  in the Minnesota force is set to  $u = 0.98$  which reproduces the  $\alpha + N$   $s$ - and  $p$ -wave phase shifts as shown in Fig. 6 of Ref. [23].

The two-body scattering  $S$  matrices of the  $\alpha + N$ ,  $t + n$ , and  $h + p$  systems are calculated by means of the microscopic  $R$ -matrix method (MRM) [24]. The combination of the MRM with the RGM has previously been applied successfully to study various light nuclei [12,20,25]. The analytic continuation of the  $S$  matrix to complex energies (ACS) [26,27] combined with the MRM [12] is employed to localize two-body resonances. Three-body resonances are localized by means of the three-body CSM [10–13]. In the CSM 15 different tempered Gaussian basis functions with range of  $b_i (= 1/\sqrt{\nu_i}) \leq 20 \text{ fm}$  are superposed in order to expand each cluster relative wave function.

Concerning the three-body calculations for  ${}^6\text{He}$ ,  ${}^6\text{Be}$ ,  ${}^5\text{H}$ , and  ${}^5\text{Be}$ , three channels are employed for the  $0^+$  state of  ${}^6\text{He}$  and  ${}^6\text{Be}$ ,

$$\begin{aligned} & \{\mu, (\ell_1, \ell_2)L, S\} \\ & = \{T, (0,0)0,0\}, \{Y, (1,1)0,0\}, \{Y, (1,1)1,1\}, \end{aligned} \quad (3)$$

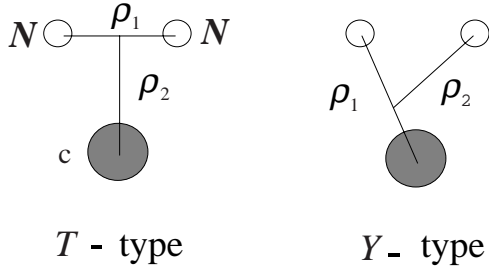
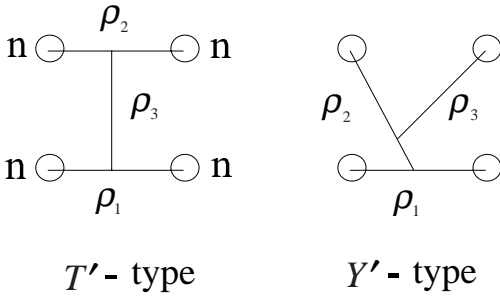
and five channels for the  $2^+$  state,

$$\begin{aligned} & \{\mu, (\ell_1, \ell_2)L, S\} \\ & = \{T, (0,2)2,0\}, \{T, (2,0)2,0\}, \{Y, (1,1)2,0\}, \\ & \{Y, (1,1)1,1\}, \{Y, (1,1)2,1\}. \end{aligned} \quad (4)$$

Seven channels are employed for the  $1/2^+$  state of  ${}^5\text{H}$  and  ${}^5\text{Be}$ ,

$$\begin{aligned} & \{\mu, (\ell_1, \ell_2)L, S_{NN}, S\} \\ & = \{T, (0,0)0,0,1/2\}, \{Y, (1,1)0,0,1/2\}, \\ & \{Y, (1,1)0,1,1/2\}, \{Y, (1,1)1,0,1/2\}, \\ & \{Y, (1,1)1,1,1/2\}, \{Y, (1,1)1,1,3/2\}, \\ & \{Y, (1,1)2,1,3/2\}, \end{aligned} \quad (5)$$

and eight channels for the  $3/2^+$  state,

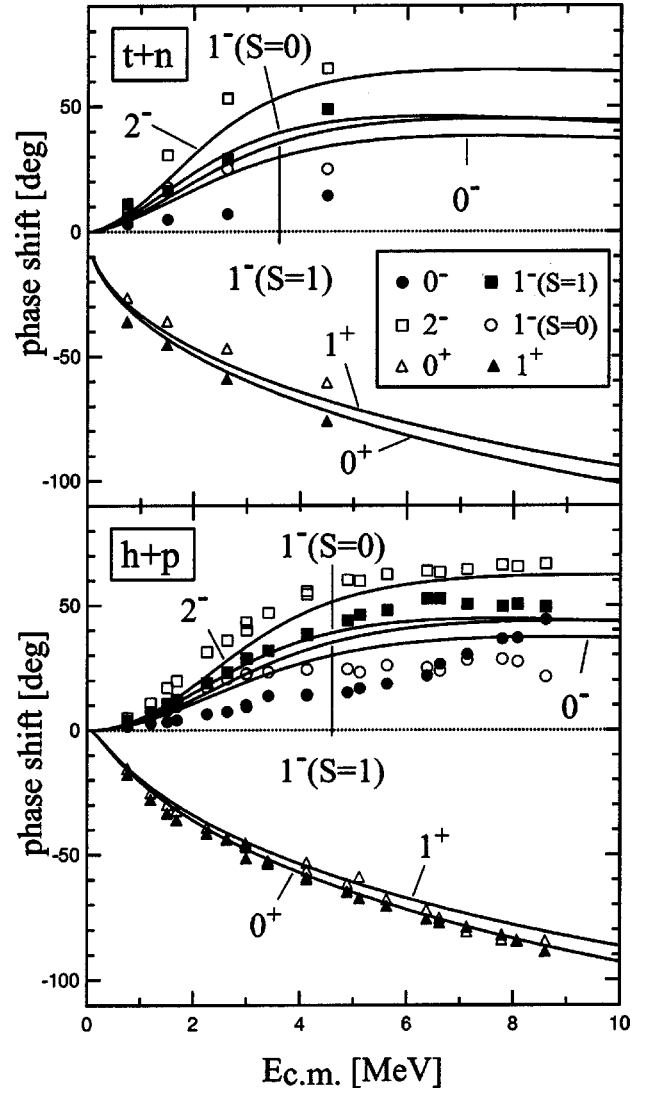
(a)  $c + N + N$  system

 (b)  $n + n + n + n$  system

 FIG. 1. Jacobi arrangements in (a) the  $c + N + N$  three-cluster system and in (b) the  $n + n + n + n$  four-body system where  $c$  stands for the  $\alpha$  particle, triton, and  $^3\text{He}$  for  $^6\text{He}$ ,  $^5\text{H}$ , and  $^5\text{Be}$ , respectively. The Jacobi coordinates are  $\rho_1$ ,  $\rho_2$ , and  $\rho_3$ .

$$\begin{aligned}
 & \{\mu, (\ell_1, \ell_2) L, S_{NN}, S\} \\
 & = \{Y, (1, 1) 0, 1, 3/2\}, \{Y, (1, 1) 1, 0, 1/2\}, \\
 & \{Y, (1, 1) 1, 1, 1/2\}, \{Y, (1, 1) 1, 1, 3/2\}, \\
 & \{T, (0, 2) 2, 0, 1/2\}, \{Y, (1, 1) 2, 0, 1/2\}, \\
 & \{Y, (1, 1) 2, 1, 1/2\}, \{Y, (1, 1) 2, 1, 3/2\},
 \end{aligned} \tag{6}$$

and five channels for the  $5/2^+$  state,

$$\begin{aligned}
 & \{\mu, (\ell_1, \ell_2) L, S_{NN}, S\} \\
 & = \{Y, (1, 1) 1, 1, 3/2\}, \{T, (0, 2) 2, 0, 1/2\}, \\
 & \{Y, (1, 1) 2, 0, 1/2\}, \{Y, (1, 1) 2, 1, 1/2\}, \\
 & \{Y, (1, 1) 2, 1, 3/2\},
 \end{aligned} \tag{7}$$

where  $T$  and  $Y$  stand for the  $(NN)c$  and  $(cN)N$  Jacobi arrangements, respectively, as shown in Fig. 1(a) with  $c$  representing for the  $\alpha$  particle in  $^6\text{He}$ , the triton in  $^5\text{H}$ , and  $^3\text{He}$  in  $^5\text{Be}$ . Finally,  $S_{NN}$  is the coupled spin of the two valence nucleons in  $^5\text{H}$  and  $^5\text{Be}$ .


 FIG. 2. Elastic scattering phase shifts of the  $h + p$  and  $t + n$  systems. Experimental data are taken from Ref. [28]. The error bars of the experimental data are omitted for clarity.

### III. RESULTS

Figure 2 shows the results for the  $s$ - and  $p$ -wave elastic scattering phase shifts for the  $t + n$  and  $h + p$  systems. Our results are compared with the experimental data [28]. The  $s$ -wave partial wave produces two states of  $J^\pi = 0^+$  and  $1^+$  and the  $p$ -wave produces four states of  $J^\pi = 0^-, 1^-(S=0), 1^-(S=1)$ , and  $2^-$ . These scattering phase shifts indicate a repulsive interaction in the  $s$  wave and an attractive interaction in the  $p$  wave as well as the  $\alpha + N$  system. The splitting between the two states ( $0^+$  and  $1^+$ ) in the  $s$  wave is very weak due to a lack of the contribution from the spin-orbit force. Also, our calculated phase shifts well reproduce the experimental  $s$ -wave phase shifts in the  $h + p$  system. In the  $t + n$  system the ordering of the two states of  $J^\pi = 0^+$  and  $1^+$  in our model is opposite to that in the experimental data. Among the six states the  $2^-$  state indicates the strongest attraction in our model as indeed is the case for the experimental data. Our calculated phase shifts of the  $2^-$  and

TABLE I. Resonance energy  $E_r$  (MeV) and width  $\Gamma_r$  (MeV) for  ${}^5\text{He}$ ,  ${}^5\text{Li}$ ,  ${}^4\text{H}$ , and  ${}^4\text{Li}$ . Energies are given relative to the respective two-body thresholds. Experimental data are taken from Ref. [2] in  ${}^5\text{He}$  and  ${}^5\text{Li}$  and from Ref. [3] in  ${}^4\text{H}$  and  ${}^4\text{Li}$ . See the text for the definition of the resonance parameters.

$J^\pi$	Cal.	$\Gamma_r$	Expt.	$\Gamma_r$
	$E_r$		$E_r$	
$^5\text{He}$				
$1/2^-$	2.03	5.43	2.07	5.57
$3/2^-$	0.78	0.64	0.798	0.648
$^5\text{Li}$				
$1/2^-$	2.86	6.31	3.18	6.60
$3/2^-$	1.63	1.24	1.69	1.23
$^4\text{H}$				
$0^-$	1.19	6.17	5.27	8.92
$1^-(S=0)$	1.32	4.72	6.02	12.99
$1^-(S=1)$	1.23	5.80	3.50	6.73
$2^-$	1.52	4.11	3.19	5.42
$^4\text{Li}$				
$0^-$	1.83	6.99	6.15	9.35
$1^-(S=0)$	1.95	5.51	6.92	13.51
$1^-(S=1)$	1.88	6.61	4.39	7.35
$2^-$	2.20	4.98	4.07	6.03

$1^-(S=1)$  states are relatively close to the experimental data whereas those of the  $1^-(S=0)$  and  $0^-$  states show a much stronger attractive interaction than in the experimental data. The splitting of the  $1^-$  state into the two different spin states ( $S=0,1$ ) is much smaller in our model than in the experimental data and the ordering of these two states is opposite to the experimental data. These disagreements are presumably attributed to the lack of the tensor term in our effective nucleon-nucleon interaction. In fact the recent GCM calculation by Descouvemont and Kharbach [7] shows that the Mertelmeier and Hofmann force [29], which includes the tensor term, enlarges the splitting and changes the order in these two  $1^-$  states and gives better agreements for the  $1^-(S=0)$  and  $0^-$  states, but this force seems to be too attractive for the  $1^-(S=1)$  state. Therefore an improved effective nucleon-nucleon interaction is required in order to reproduce these phase shifts more accurately, but constructing a new effective nucleon-nucleon interaction is out of the scope in present paper.

Table I shows the two-body resonance parameters of  ${}^4\text{H}$  and  ${}^4\text{Li}$  together with the results for  ${}^5\text{He}$  and  ${}^5\text{Li}$ . The resonance parameters derived from the ACS in our model are defined as position of the  $S$ -matrix pole on the complex energy plane. The experimental data for  ${}^5\text{He}$  and  ${}^5\text{Li}$  in Table I are derived from the extended  $R$ -matrix prescription based on the complex pole of the  $S$ -matrix [2]. Thus, there is naturally good agreement between our results for  ${}^5\text{He}$  and  ${}^5\text{Li}$  and the experimental data. However, the experimental data of  ${}^4\text{H}$  and  ${}^4\text{Li}$  in Table I are obtained by the conventional  $R$  matrix or Breit-Wigner fit to the peak of the cross section involving these nuclei [3]. It is known that the resonance parameters derived from this way may be different from

those based on the position of the  $S$ -matrix pole. These different definitions often lead to some discrepancies in resonance parameters, especially for broad resonance states. For example, this sort of discrepancies in  ${}^5\text{He}({}^5\text{Li})$  can be found in Tables 5.1 and 5.2 (5.3 and 5.4) of Ref. [2] and in Table I of Ref. [27]. In our model the  $2^-$  state has the smallest width among the  $p$ -wave resonances in agreement with the experimental data, but this model state has a higher resonance energy than the other three resonances whereas it is lowest resonance in the experimental data [3]. However, the differences between the resonance energies for these four states in our model are small and consequently we can be confident that the  $2^-$  state in  ${}^4\text{H}$  ( ${}^4\text{Li}$ ) will be the most important for the explaining the experimentally observed  ${}^5\text{H}({}^5\text{Be})$  resonances. The width of the  $1^-$  state with  $S=0$  is much smaller in our model than the experimental width and is smaller than that of the  $1^-$  state with  $S=1$  in contrast to the experimental data. In our model the resonance energies of the four  $p$ -wave states are concentrated within a small energy range but experimentally the resonance energies of the  $0^-$  and  $1^-(S=0)$  states are 2–3 MeV higher than those of the  $2^-$  and  $1^-(S=1)$  states. In addition the resonance energies of the  $2^-$  and  $1^-(S=1)$  states in our model are 1.7–2.5 MeV lower than those in the experimental data.

Table II shows the three-body resonance parameters for  ${}^5\text{H}$ ,  ${}^5\text{Be}$ ,  ${}^6\text{He}$ , and  ${}^6\text{Be}$  where these resonance states are localized by the three-body CSM. Since the many-body problem is solved approximately using the finite number of Gaussian basis set, it is known that the complex resonance eigenvalue of the complex rotated Hamiltonian has some dependences on the basis set and the rotational angle [30]. As usually in the CSM, the stationary point of the  $\theta$  trajectory [30] is regarded as the resonance position and in addition the resonance parameters given in Table II are sufficiently convergent values in the dimension of the basis set ( $n$  trajectory [30]). In the present study, the resonance parameters are determined by only single basis set in order to save computing time, but our test calculation shows that other choices of the basis set give only insignificant difference on the resonance parameters. Figure 3 shows, for example, eigenvalues of the complex rotated Hamiltonian of the  $1/2^+$  state in  ${}^5\text{H}$  with a rotational angle of  $\theta=0.46$  rad. There is evidently one resonance eigenvalue (white circle) separated from the continuum eigenvalues (solid circle) where the resonance energy  $E_r$  and width  $\Gamma_r$  are related to the complex energy by  $E = E_r - i\Gamma_r/2$ . The results for  ${}^6\text{He}$  and  ${}^6\text{Be}$  give reasonable agreement with the experimental data. The  $0^+$  ground state of  ${}^6\text{He}$  with the three-body model has a well-known underbinding problem [4] and accordingly the resonance energy of the  $0^+$  state in  ${}^6\text{Be}$  is a little higher in our model than the experimental energy, with consequently a little larger width. In contrast, the resonance energy of the  $2^+$  excited state is a little lower than the experimental energy and the width is a little smaller than the experimental width in both  ${}^6\text{He}$  and  ${}^6\text{Be}$  [10]. Tiny differences of the resonance parameters for the  $2^+$  state between our results and those in Ref. [10] might arise from an enlargement of the basis set in the present model. The total angular momentum of the ground state in both  ${}^5\text{H}$  and  ${}^5\text{Be}$  in our model is  $1/2^+$  corresponding



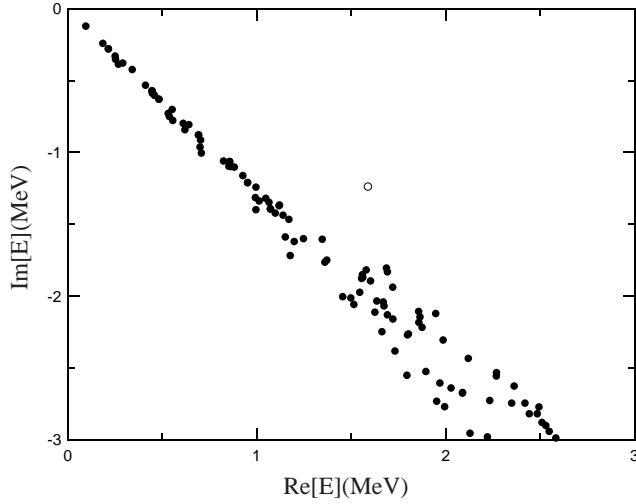


FIG. 3. Complex eigenvalues in the CSM for the  $1/2^+$  state in  ${}^5\text{H}$ . The rotation angle is  $\theta=0.46$  rad. The open circle corresponds to the complex eigenvalue of the resonance state.

to the  $0^+$  ground state of  ${}^6\text{He}$ . The widths of these ground states are 2.48 MeV in  ${}^5\text{H}$  and 3.62 MeV in  ${}^5\text{Be}$  and these widths are naturally much broader than that of the ground state of  ${}^6\text{Be}$ . Our result for the  $1/2^+$  state in  ${}^5\text{H}$  ( $E_r = 1.59$  MeV,  $\Gamma_r = 2.48$  MeV) is quite close to the recent experimental data by Korshennikov *et al.*,  $E_r = 1.7 \pm 0.3$  MeV with  $\Gamma_r = 1.9 \pm 0.4$  MeV [14]. It should be noted that these experimental resonance parameters are derived from the Breit-Wigner fit to a peak in the  ${}^5\text{H}$  spectrum whereas the resonance parameters in the CSM are based on the complex  $S$ -matrix pole. As it is already mentioned above, these different definitions of the resonance parameters can lead to some discrepancies in the resonance parameters, especially for broad resonances. The Coulomb displacement energy in the  $1/2^+$  state of  ${}^5\text{H}$ - ${}^5\text{Be}$  is 1.56 MeV which is smaller than the 2.18 MeV for the  $0^+$  state in  ${}^6\text{He}$ - ${}^6\text{Be}$ , simply reflecting the different number of charges in the core. Our model gives two excited states with total angular momenta  $3/2^+$  and  $5/2^+$  and both states have very large widths.

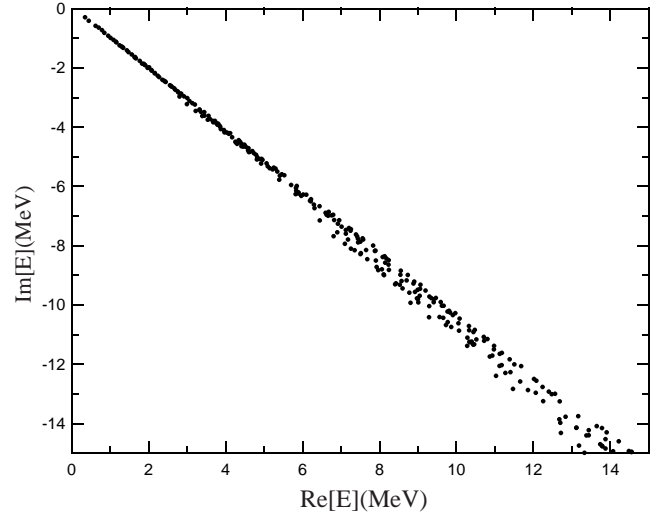


FIG. 4. Complex eigenvalues in the CSM for the  $0^+$  state of the  $n+n+n+n$  system. The rotation angle is  $\theta=0.4$  rad.

The  $5/2^+$  state is lower than the  $3/2^+$  state but the splitting of these two states is very small (about 0.1 MeV). As well as the two  $1^-$  states in  ${}^4\text{H}$ , this splitting is possibly enlarged by the inclusion of the tensor term in the effective nucleon-nucleon interaction. The excitation energies are  $E_x = 1.31$ – $1.45$  MeV for these states which, as expected, are not very different from the  $2^+$  energies of  $E_x = 1.3$  MeV in  ${}^6\text{He}$  and  $E_x = 1.16$  MeV in  ${}^6\text{Be}$  according to our model.

We now apply the same effective nucleon-nucleon interaction to discuss the tetra-neutron. However, since two neutrons do not form a bound state, it is no longer valid to assume a core cluster inside the tetra-neutron as was done for  ${}^6\text{He}$  and  ${}^5\text{H}$ . Therefore we should solve the four-body ( $n+n+n+n$ ) problem and here we apply the four-body complex scaling method to explore the possibility of a four-neutron resonance. In this paper we consider only the  $0^+$  state that is expected as the ground state, since two neutrons occupy the  $s_{1/2}$  orbit and other two neutrons occupy the  $p_{3/2}$  orbit in a shell model configuration. Owing to a computer limitation, we compromise by taking into account only three

TABLE II. Resonance energy  $E_r$  (MeV) and width  $\Gamma_r$  (MeV) of  ${}^6\text{He}$ ,  ${}^6\text{Be}$ ,  ${}^5\text{H}$ , and  ${}^5\text{Be}$ . Energies are given relative to the respective three-body thresholds. Values within the parentheses indicate the experimental data taken from Ref. [2] for  ${}^6\text{He}$  and  ${}^6\text{Be}$  and from Ref. [14] for  ${}^5\text{H}$ . See the text for the definition of the resonance parameters.

$J^\pi$	$E_r$	$\Gamma_r$	$E_r$	$\Gamma_r$
	${}^6\text{He}$		${}^6\text{Be}$	
$0^+$	-0.66 (-0.973)		1.52 (1.3711)	0.16 (0.092 $\pm$ 0.006)
$2^+$	0.64 (0.824 $\pm$ 0.025)	0.04 (0.113 $\pm$ 0.020)	2.68 (3.04 $\pm$ 0.05)	0.74 (1.16 $\pm$ 0.06)
	${}^5\text{H}$		${}^5\text{Be}$	
$1/2^+$	1.59 (1.7 $\pm$ 0.3)	2.48 (1.9 $\pm$ 0.4)	3.15	3.62
$3/2^+$	3.0	4.8	4.6	6.3
$5/2^+$	2.9	4.1	4.5	5.6

channels which relate to the three channels used in the ground state of  ${}^6\text{He}$ , given in Eq. (3). These three channels are

$$\{\mu, (\ell_2, \ell_3)L, S\} \\ = \{T', (0,0)0,0\}, \{Y', (1,1)0,0\}, \{Y', (1,1)1,1\}, \quad (8)$$

where  $T'$  and  $Y'$  stand for the  $(nn)(nn)$  and  $((nn)nn)$  Jacobi arrangements, respectively, as shown in Fig. 1(b). The orbital angular momentum  $\ell_1$  is set to zero and consequently the two neutrons connected by  $\mathbf{p}_1$  are allowed to couple to zero spin due to the Pauli principle. These two neutrons can be regarded as the two neutrons occupying the  $s_{1/2}$  orbit. The Minnesota force is constructed to reproduce the experimental scattering lengths and effective ranges of the  $s$ -wave  $n+p$  triplet and  $p+p$  singlet states [21] and gives a virtual state at  $E = -0.13 - i0.0$  MeV for the  $s$ -wave  $n+n$  singlet state. Since no cluster structure is any longer assumed, it is desirable to employ a realistic nucleon-nucleon interaction, but a search of the four-body resonance with such a complicated force would give rise to enormous difficulties and is not feasible with the CSM. In addition, the aim of this paper is to discuss the four-neutron system in a consistent way with  ${}^6\text{He}$  and  ${}^5\text{H}$ . Ten tempered Gaussian basis functions are superposed on each Jacobi coordinate, with ranges of  $b_1 \leq 15$  fm and  $b_2, b_3 \leq 20$  fm. We have explored the  $0^+$  state up to  $\theta = 0.5$  with this condition but have found no evidence for such a four-neutron resonance within the present model. Figure 4 shows the eigenvalues of the complex rotated Hamiltonian with  $\theta = 0.4$ , for example. The conclusion is that the present model does not produce a four-neutron resonance or, alternatively, any such resonance must have a very broad width which cannot be identified over the range of  $0 < \theta \leq 0.5$ , even if it exists. It may also be observed that, since the CSM does not work for the virtual state, if the virtual state-like property of two neutrons persists inside the tetra-neutron (if it exists), then as a consequence the CSM might not work to identify such a four-body resonance. Therefore further,

more elaborate and sophisticated calculations are required to confirm the above result, but that is beyond the scope of the present work.

#### IV. CONCLUSIONS

We have calculated the resonance states of  ${}^5\text{H}$  and  ${}^5\text{Be}$  using the same effective nucleon-nucleon interaction as for  ${}^6\text{He}$  and with a consistent model space. The present effective nucleon-nucleon interaction, which can reproduce the experimental low energy  $s$ - and  $p$ -wave  $\alpha+N$  phase shifts, reasonably reproduces the experimental low energy  $h+p$  and  $t+n$  phase shifts. Our model gives the  $1/2^+$  state as the ground state of  ${}^5\text{H}$  with a resonance energy and a rather broad width that are both quite close to the recent experimental data [14]. Further, it predicts two excited states ( $3/2^+$  and  $5/2^+$ ) with very broad widths and a vanishingly small energy splitting but the latter is possibly enlarged by an additional tensor term in the effective nucleon-nucleon interaction. The mirror nucleus  ${}^5\text{Be}$  has also been calculated and it has a similar spectrum. To give more accurate and reliable resonance positions of  ${}^5\text{H}$  and  ${}^5\text{Be}$  theoretically, an improvement of the effective nucleon-nucleon interaction is required to reproduce accurately the low energy properties of the  $t+n$ ,  $h+p$  and  $\alpha+N$  systems simultaneously.

Finally, the same effective nucleon-nucleon interaction has been used to search for a  $0^+$  resonance state of the tetra-neutron ( ${}^4n$ ) system with a restricted number of basis states. The four-body  $n+n+n+n$  complex scaling method gives no evidence of such a resonance state within the present model.

#### ACKNOWLEDGMENTS

The author acknowledges Dr. P. Descouvemont and Dr. W. N. Catford for helpful comments and reading the manuscript. This work was funded by the CHARISSA Collaboration Grant No. GR/R38927/01 by the EPSRC.

- 
- [1] I. Tanihata, J. Phys. G **22**, 157 (1996).
  - [2] D.R. Tilley, C.M. Cheves, J.L. Godwin, G.M. Hale, H.M. Hofmann, J.H. Kelley, C.G. Sheu, and H.R. Weller, Nucl. Phys. A **708**, 3 (2002).
  - [3] D.R. Tilley, H.R. Weller, and G.M. Hale, Nucl. Phys. A **541**, 1 (1992).
  - [4] A. Cs    , Phys. Rev. C **48**, 165 (1993).
  - [5] K. Arai, Y. Suzuki, and R.G. Lovas, Phys. Rev. C **59**, 1432 (1999).
  - [6] N.B. Shul'gina, B.V. Danilin, L.V. Grigorenko, M.V. Zhukov, and J.M. Bang, Phys. Rev. C **62**, 014312 (2000).
  - [7] P. Descouvemont and A. Kharbach, Phys. Rev. C **63**, 027001 (2001).
  - [8] Y.K. Ho, Phys. Rep. **99**, 1 (1993).
  - [9] N. Moiseyev, Phys. Rep. **302**, 212 (1998).
  - [10] A. Cs    , Phys. Rev. C **49**, 3035 (1994).
  - [11] S. Aoyama, S. Mukai, K. Kat  , and K. Ikeda, Prog. Theor. Phys. **93**, 99 (1995); **94**, 343 (1995).
  - [12] K. Arai, Y. Ogawa, Y. Suzuki, and K. Varga, Phys. Rev. C **54**, 132 (1996); K. Arai, P. Descouvemont, D. Baye, and W. Catford, Phys. Rev. C **68**, 014310 (2003).
  - [13] R. Pichler, H. Oberhummer, A. Cs    , and S.A. Moszkowski, Nucl. Phys. A **618**, 55 (1997).
  - [14] A.A. Korshennikov *et al.*, Phys. Rev. Lett. **87**, 092501 (2001).
  - [15] F.M. Marqu  s *et al.*, Phys. Rev. C **65**, 044006 (2002).
  - [16] A. Cs    , H. Oberhummer, and R. Pichler, Phys. Rev. C **53**, 1589 (1996), and references therein.
  - [17] N.K. Timofeyuk, J. Phys. G **29**, L9 (2003), and references therein.
  - [18] K. Wildermuth and Y. C. Tang, *A Unified Theory of the Nucleus* (Vieweg, Braunschweig, 1977).
  - [19] K. Langanke, in *Advances in Nuclear Physics*, edited by J. W. Negele and E. Vogt (Plenum, New York, 1994), Vol. 21, p. 85.

- [20] K. Arai, P. Descouvemont, and D. Baye, Phys. Rev. C **63**, 044611 (2001).
- [21] D.R. Thompson, M. LeMere, and Y.C. Tang, Nucl. Phys. **A286**, 53 (1977).
- [22] I. Reichstein and Y.C. Tang, Nucl. Phys. **A158**, 529 (1970).
- [23] K. Arai and A.T. Kruppa, Phys. Rev. C **60**, 064315 (1999).
- [24] D. Baye, P.-H. Heenen, and M. Libert-Heinemann, Nucl. Phys. **A291**, 230 (1977).
- [25] K. Fujimura, D. Baye, P. Descouvemont, Y. Suzuki, and K. Varga, Phys. Rev. C **59**, 817 (1999).
- [26] A. Csóto, R.G. Lovas, and A.T. Kruppa, Phys. Rev. Lett. **70**, 1389 (1993).
- [27] A. Csóto and G.M. Hale, Phys. Rev. C **55**, 536 (1997).
- [28] T.A. Tombrello, Phys. Rev. **138**, B40 (1965); Phys. Rev. **143**, 772 (1966).
- [29] T. Mertelmeier and H.M. Hofmann, Nucl. Phys. **A459**, 387 (1986).
- [30] A.T. Kruppa, R.G. Lovas, and B. Gyarmati, Phys. Rev. C **37**, 383 (1988); A.T. Kruppa and K. Katō, Prog. Theor. Phys. **84**, 1145 (1990).